MOLECULAR AND CELLULAR BIOLOGY, May 2005, p. 3715–3725 Vol. 25, No. 9
0270-7306/05/$08.00+0 doi:10.1128/MCB.25.9.3715–3725.2005

Interaction of BAG1 and Hsp70 Mediates Neuroprotectivity and Increases Chaperone Activity†

Jan Liman,[1]‡ Sundar Ganesan,[2]‡ Christoph P. Dohm,[1] Stan Krajewski,[3] John C. Reed,[3] Mathias Bähr,[1] Fred S. Wouters,[2]*‡ and Pawel Kermer[1]*‡

Neurologische Klinik, Universität Göttingen,[1] and Cell Biophysics Group, European Neuroscience Institute Göttingen,[2] Göttingen, Germany, and The Burnham Institute, La Jolla, California[3]

Received 17 September 2004/Returned for modification 20 October 2004/Accepted 19 January 2005

It was recently shown that Bcl-2-associated athanogene 1 (BAG1) is a potent neuroprotectant as well as a marker of neuronal differentiation. Since there appears to exist an equilibrium within the cell between BAG1 binding to heat shock protein 70 (Hsp70) and BAG1 binding to Raf-1 kinase, we hypothesized that changing BAG1 binding characteristics might significantly alter BAG1 function. To this end, we compared rat CSM14.1 cells and human SHSY-5Y cells stably overexpressing full-length BAG1 or a deletion mutant (BAGΔC) no longer capable of binding to Hsp70. Using a novel yellow fluorescent protein-based foldase biosensor, we demonstrated an upregulation of chaperone in situ activity in cells overexpressing full-length BAG1 but not in cells overexpressing BAGΔC compared to wild-type cells. Interestingly, in contrast to the nuclear and cytosolic localizations of full-length BAG1, BAGΔC was expressed exclusively in the cytosol. Furthermore, cells expressing BAGΔC were no longer protected against cell death. However, they still showed accelerated neuronal differentiation. Together, these results suggest that BAG1-induced activation of Hsp70 is important for neuroprotectivity, while BAG1-dependent modulation of neuronal differentiation in vitro is not.

Bcl-2-associated athanogene 1 (BAG1) is the first identified member of the BAG protein family, which consists of at least six different members identified in mammals to date. With the exception of BAG5, all BAG family members share the highly conserved BAG domain near the C terminus (37). The BAG family proteins differ in various other domains, allowing interactions with cellular binding partners and differential subcellular targeting. BAG1 binds to the ATPase domain of the 70-kDa heat shock protein (Hsp70) and its cognate protein Hsc70 (hereafter referred to as Hsp70), which are chaperones, through the BAG domain, thereby serving as a cochaperone and modulating chaperone activity (37–39). Moreover, multiple functions of BAG1 have been proposed; these include interaction and activation of the serine/threonine-specific protein kinase Raf-1 via its N-terminal domain (34, 45) as well as binding to steroid hormone and other receptors (2, 45, 50). Many studies dealing with BAG1 function revealed that it increases resistance to death stimuli when overexpressed in vitro, including in neuronal cells (19, 31, 35, 38, 43, 44). The neuroprotective effects were confirmed in vivo with transgenic mice overexpressing BAG1. Explanted primary neurons displayed increased resistance against glutamate toxicity. Moreover, BAG1 proved to be neuroprotective against stroke induced by middle cerebral artery occlusion in these mice (18).

Apart from its antiapoptotic effects, BAG1 also accelerates differentiation when overexpressed in neurons (19). In fact, $BAG1^{-/-}$ mice die during embryogenesis due to failed neurogenesis (46; unpublished observations), indicating an important role for the BAG1 gene in neuronal differentiation, neuronal survival, or both in vivo. It has been proposed that these multifunctional properties of BAG1 depend on its interactions with cellular binding partners. For example, there is evidence for a balance between BAG1 binding to Raf-1 or Hsp70 (34). This scenario raises the possibility that BAG1 promotes cell growth by binding to and stimulating the activity of Raf-1, whereas its antiapoptotic effects are modulated by its interaction with Hsp70. Thus, BAG1 may serve as a molecular switch, encouraging cells to proliferate and differentiate under permissive conditions and allowing survival under nonpermissive conditions (34, 37, 45). Moreover, conflicting data have been reported regarding the modulation of chaperone activity by BAG1. While BAG1 was originally characterized as an inhibitor of Hsp70 activity in vitro, recent evidence suggests that BAG1 can act as a stimulatory or an inhibitory cochaperone, depending on cell type, cofactor expression, and concentration (10, 41).

To resolve the question of how the interaction of BAG1 and Hsp70 influences chaperone activity in single neuronal cells, we generated a chaperone-dependent yellow fluorescent protein (YFP) folding mutant (cdYFP) and measured its refolding in rat nigral CSM14.1 and human SHSY-5Y neuroblastoma cells stably overexpressing full-length BAG1 or a truncated BAG1 construct (BAGΔC) lacking the ability to bind Hsp70. Cells overexpressing BAGΔC were also characterized and compared to those containing full-length BAG1 (19) with re-

* Corresponding author. Mailing address for Fred S. Wouters: Cell Biophysics Group, European Neuroscience Institute Göttingen, Waldweg 33, 37075 Göttingen, Germany. Phone: 0049-551-3912368. Fax: 0049-551-3912346. E-mail: fred.wouters@gwdg.de. Mailing address for Pawel Kermer: Neurologische Klinik, Universität Göttingen, Robert-Koch-Str. 40, 37075 Göttingen, Germany. Phone: 49-551-394927. Fax: 49-551-3914302. E-mail: pkermer@gwdg.de.

† Supplemental material for this article may be found at http://mcb.asm.org/.

‡ J.L., S.G., F.S.W., and P.K. contributed equally to this work.

gard to neuronal differentiation and susceptibility to apoptosis. Here we show for the first time, using intact cells of different species, that BAG1 is a potent inducer of Hsp70 chaperone activity in neurons and that BAG1 neuroprotectivity is dependent on this cochaperone effect. In contrast, the ability of BAG1 to promote neuronal differentiation is independent of Hsp70 binding and cochaperone activity.

MATERIALS AND METHODS

Cloning of constructs and development of cdYFP. Detailed information on constructs can be found in the supplemental material. cdYFP was generated by a single round of random mutagenesis of enhanced YFP, and folding-impaired mutants were selected by visual inspection of the bacterial colony phenotype. The selected mutants, showing fluorescent and nonfluorescent pools of bacteria within one colony, were further selected on the basis of early folding and high fluorescence recovery criteria. The remaining mutants were subjected to bacterial chaperone induction to gauge the dynamic range of the folding response shown by fluorescence and were purified for further spectroscopic characterization.

Fluorescence-based folding assay. Cell lines (CHO, CSM14.1, and SHSY-5Y) grown to ±40% confluence on 25-mm coverslips in six-well tissue culture plates were transfected with 0.5 μg of cdYFP or hemagglutinin (HA)-cdYFP per well of a six-well tissue culture plate by using magnet-assisted transfection according to the supplier's protocol (IBA GmbH, Göttingen, Germany) and were allowed to express the protein overnight. Cells were fixed with 4% formaldehyde in phosphate-buffered saline (PBS) for 10 min, washed three times with PBS, and quenched for 10 min with 50 mM Tris (pH 7.5)–100 mM NaCl. For the quantitation of folding efficiency, pECFP (BD Biosciences Clontech) was coexpressed with cdYFP or cells expressing HA-cdYFP were subjected to anti-HA antibody immunofluorescence analysis after permeabilization of fixed cells with 0.1% Triton X-100 in PBS for 20 min. Cells were blocked with 5% bovine serum albumin in PBS prior to incubation for 2 h with a 1:1,000 dilution of the primary anti-HA monoclonal antibody (Covance Research Products, Columbia, Mo.) and subsequent incubation for 1 h with a 1:300 dilution of the Cy5-labeled goat anti-mouse secondary antibody (Jackson Laboratories, Bar Harbor, Maine). Cells were mounted in Mowiol. Three 5-min washes with PBS were performed between the steps.

Cells were imaged by using a Leica SP2 confocal laser scanning microscope equipped with an AOBS acoustooptical beam splitter, allowing custom selection of emission detection bands. For the detection of YFP fluorescence, cells were excited with the 514-nm argon laser line, and emission was recorded at 525 to 600 nm. For the detection of cyan fluorescent protein (CFP) fluorescence, excitation was done with the 458-nm argon laser line, and emission was recorded at 465 to 520 nm. For the detection of Cy5 fluorescence, excitation was done with the 633-nm HeNe laser line, and emission was recorded at 640 to 750 nm. Photomultiplier tube gains were kept constant for each emission range throughout the acquisitions. CFP or Cy5 fluorescence serves as an inert concentration reference for the total concentration of cdYFP. The folding efficiency was retrieved by simple image arithmetic (YFP fluorescence/reference fluorescence) by using ImageJ software (http://rsb.info.nih.gov/ij/). The image intensity values were corrected for the various laser power settings needed to obtain proper photon statistics under the various conditions. The laser power settings were shown to be linearly calibrated by comparison of the fluorescence intensities of fluorescent beads at various settings. The ratio images were masked based on threshold fluorescence intensities in the CFP or Cy5 channel to remove noise in the noncellular background. The folding ratios were always normalized to the first, partial folding peak in wild-type cells (see Results), so that the effects on the folding response were expressed in units of native folding activity. Folding ratio frequency histograms were obtained from masked images of 10 cells for each condition, unless indicated otherwise. For the Cy5 masking, the nucleus was also masked on the basis of its lower Cy5 signals, which represent incomplete penetration of the labeled antibody, a situation that would alter the folding statistics. Folding ratio frequency histograms were analyzed by using the Igor analysis package. Individual histograms were summed, and cumulative histograms were normalized to the integrated counts, i.e., to the number of observed pixels per experimental data set.

Stable transfection. The rat nigrostriatal cell line CSM14.1, immortalized by introduction of the temperature-sensitive simian virus 40 large T antigen, and SHSY-5Y cells were maintained in Dulbecco's modified Eagle's medium (PAA, Pasching, Austria) supplemented with 10% fetal bovine serum (PAA), 1 mM L-glutamine, 100 U of penicillin/ml, and 100 μg of streptomycin sulfate/ml at either 32°C (permissive temperature) or 39°C (nonpermissive temperature) for CSM14.1 cells (49) and at 37°C for SHSY-5Y cells. For stable transfection, 50 to 70% confluent cells in six-well plates were incubated with Lipofectamine 2000 according to the supplier's protocol (Invitrogen, Carlsbad, Calif.) in serum-free medium containing 3 μg of pcDNA3.1(+) plasmid DNA (Invitrogen) expressing a myc tag-encoding fragment subcloned with HindIII/EcoRI and the BAGΔC DNA subcloned with EcoRI/XhoI, representing a 5:1 ratio of specific plasmid to puromycin resistance plasmid (pBabe-puro). After 3 h at 32°C, serum-containing medium was added, and the cells were incubated overnight. SHSY-5Y cells were transfected only with 3 μg of pCI-neo plasmid DNA (Promega, Madison, Wis.) containing a FLAG tag subcloned with XhoI/SalI and mBAG1 DNA subcloned with SalI/NotI. Finally, the transfection agent was replaced with medium containing 10% fetal bovine serum. Selection with 4 μg of puromycin (CSM14.1 cells) or 250 μg of G418 (SHSY-5Y cells) in complete medium was started on the next day. After 5 days, cells were placed in 96-well plates (0.5 cell per well) with selection medium; 3 to 4 weeks later, wells containing single clones were identified by light microscopy. Cells were transferred to larger plates for expansion and further processing.

Empty vector-transfected cells as well as nontransfected CSM14.1 cells, both referred to as wild-type cells, served as control groups for the cell experiments.

Cell death, cell division assays, and measurement of neurite outgrowth. Cell death in the various stable cell lines was induced with either staurosporine or thapsigargine. For staurosporine-induced cell death, cells were plated on 96-well plates at a density of 10,000 cells per well and maintained at 32°C for 1 day prior to the experiment. Next, staurosporine was added at various concentrations (0.05, 0.1, and 1 μM) and incubated for 48 h. For thapsigargine-induced cell death, cells were plated on 96-well plates at a density of 5,000 cells per well, maintained at 39°C for 8 days, and incubated with 3 μM thapsigargine for 48 h.

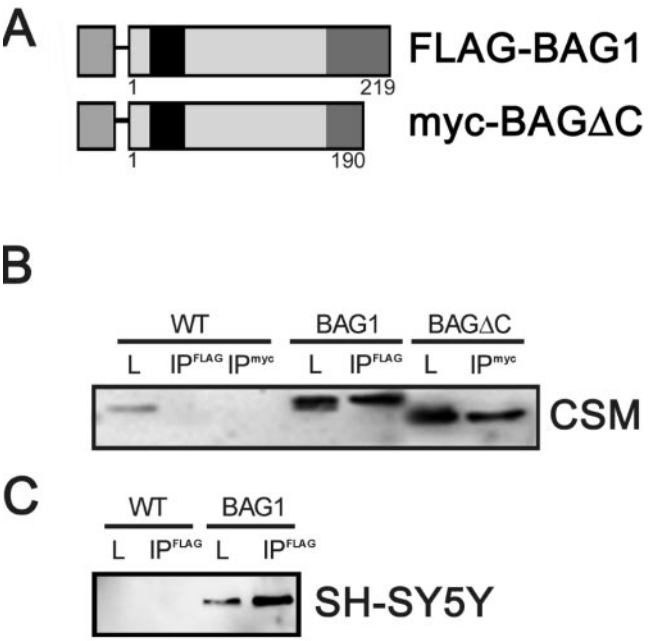

FIG. 1. BAG constructs. (A) The BAGΔC mutant was generated by deletion of 29 C-terminal residues of p29 mouse BAG1, truncating the BAG domain. BAGΔC was N-terminally tagged with a myc epitope tag; full-length BAG1 was N-terminally tagged with a FLAG epitope tag. The N-terminal ubiquitination domain is represented by a black box. (B) Immunoprecipitation (IP) with respective antibodies against the epitope tags and development with an antibody against BAG1 reveal strong expression of stably transfected proteins. Endogenous BAG1 present in all protein lysates served as an endogenous control. CSM, CMS14.1 cells; WT, wild type. (C) Stable expression of BAG1 in human SH-SY5Y cells. Note that the BAG antibody did not react with endogenous human BAG1.

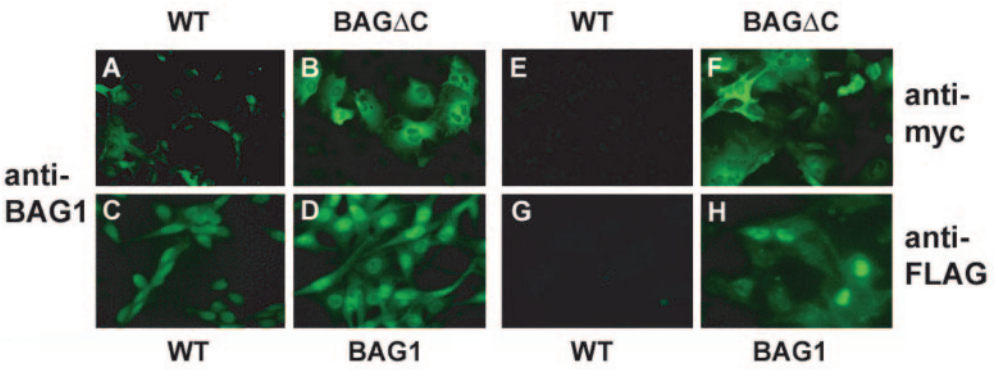

FIG. 2. Stable expression of BAGΔC. Representative photomicrographs were taken at magnifications of ×152 (A, B, E, and F) and ×304 (C, D, G, and H). Wild-type (WT) cells (A, C, E, and G) and cells overexpressing BAGΔC (B and F) or BAG1 (D and H) were stained with anti-BAG antiserum (A to D), anti-myc antibody (E and F), or anti-FLAG antibody (G and H). Note the cytoplasmic distribution of BAGΔC. The baseline fluorescence in wild-type cells stained with anti-BAG antiserum (A and C) is caused by the endogenous expression of BAG1, which is not present in cells stained with anti-myc antibody (E) or anti-FLAG antibody (G).

Cell survival was assessed by crystal violet staining. Data collection was performed with a spectrophotometer at a wavelength of 550 nm.

Doubling times were determined during logarithmic growth on 24-well plates. A total of 10^4 cells were plated, and daily cell counts were obtained with a trypan blue exclusion assay for 1 week. All experiments were repeated at least six times.

The length of outgrowing neurites was assessed on day 8 at 39°C in three independent experiments with 70 randomly picked cells in each group by using KS400 software (Zeiss, Oberkochen, Germany). Statistics were performed with a two-tailed Student *t* test.

To assess Hsp70 neuroprotectivity, cells were transiently transfected with rat pECFP-C1-Hsp70 or pECPF-C1 (BD Biosciences, Franklin Lakes, N.J.) as described above 24 h prior to staurosporine treatment (see above). Vital and dead cells were counted under a fluorescence microscope in a blinded fashion by two investigators.

For the investigation of caspase activation in our model, cells were treated with 0.1 μM staurosporine. After 12 h of incubation, caspase 3 activity was measured by using a Caspase Glo 3/7 detection system (Promega) according to the manufacturer's protocol.

Immunoblot and immunofluorescence analyses. Cell lysates were prepared at various times with HKME buffer as described previously (19). Briefly, proteins were resolved by sodium dodecyl sulfate-polyacrylamide gel electrophoresis and transferred to nitrocellulose membranes. Blocking was done with 5% skim milk–2% bovine serum albumin in 10 mM Tris (pH 7.5)–142 mM NaCl–0.1% Tween 20 at room temperature for 2 h. Next, the blots were incubated in the same solution with polyclonal primary antibody BUR1680 against the BAG protein (1:1,000; described in detail in references 19 and 38) as well as monoclonal antibodies against myc (1:1,000; Santa Cruz Biotechnology, Santa Cruz, Calif.) and phosphorylated mitogen-activated protein kinase Erk1/2 and mitogen-activated protein kinase Erk1/2 (1:1,000; Cell Signaling, Beverly, Mass.), followed by horseradish peroxidase-conjugated anti-mouse or anti-rabbit immunoglobulin G (Bio-Rad, Hercules, Calif.) secondary antibodies. Bound antibodies were visualized by using an enhanced chemiluminescence detection system (Amersham, Freiburg, Germany). The binding of BAG1 to Hsp70 as well as the lack of Hsp70 binding by BAGΔC was shown previously multiple times (32, 34, 37).

For immunofluorescence analysis, wild-type cells and those stably transfected with BAGΔC were trypsinized and placed on chamber slides. Cells were maintained at either 32 or 39°C until further processing. After various times, cells were washed with PBS and fixed in PBS containing 4% paraformaldehyde for 10 min at room temperature, followed by several washes with PBS. Permeabilization was performed with 0.5% Triton X-100–PBS for 10 min; subsequent preblocking was done with PBS containing 2% normal goat serum. Cells were incubated in blocking solution containing the following primary antibodies: BUR1680 (1:1,000), anti-myc (1:250; Santa Cruz), and anti-NeuN (1:200; Chemicon, Temecula, Calif.). After three washes with PBS and incubation with fluorescein isothiocyanate- or Cy3-conjugated secondary anti-mouse or anti-rabbit antibodies (1:500; Dako, Glostrup, Denmark) for 1 h at room temperature, the slides were covered with Vectashield mounting medium containing 1.5 μg of 4′,6′-diamidino-2-phenylindole (DAPI; Vector Laboratories, Burlingame, Calif.)/ml and sealed with Cytoseal 60 mounting medium (Stephens Scientific, Riverdale, N.J.).

RESULTS

Overexpression of BAG1 and BAGΔC in neuronal cells. The C-terminal region of the BAG1 protein contains the Hsp70 binding BAG domain. We therefore compared the effects of full-length BAG1 and of a mutant lacking this C-terminal domain. CSM14.1 neuronal cells (51) were stably transfected with a plasmid encoding full-length BAG1 (19) or myc-tagged mouse BAGΔC (residues 1 to 190 of full-length BAG1) driven by the cytomegalovirus promoter (Fig. 1A). Moreover, SHSY-5Y cells were stably transfected with full-length BAG1. By immunoblotting, we found strong expression of BAGΔC in CSM14.1 cells (Fig. 1B) as well as BAG1 in SHSY-5Y cells (Fig. 1C), with BAGΔC migrating in gels slightly faster than endogenous BAG1 (Fig. 1B).

Immunofluorescence microscopy revealed an extensively cytosolic localization in cells stably overexpressing BAGΔC (Fig. 2B and F). This result was markedly different from that obtained for wild-type cells (Fig. 2A and C) and cells overexpressing full-length BAG1, where we observed both nuclear expression and cytosolic expression in undifferentiated cells under control conditions (Fig. 2D and H). No staining was observed in CSM14.1 control cells when anti-myc antibody was used (Fig. 2E and G). Omission of the first antibody served as an additional control (data not shown).

Chaperone foldase activity sensor cdYFP. To assess the impact of BAG1 and BAGΔC on chaperone activity in intact cells, we generated cdYFP. This chaperone foldase activity sensor was identified from a random mutagenesis screen of YFP by visual inspection of the bacterial phenotype of the colonies (see the supplemental material). The typical and obvious heterogeneous distribution of fluorescence in the colonies expressing foldase-sensitive mutants (Fig. 3A) is explained by the spontaneous upregulation of the bacterial chaperone program due to the presence of high concentrations of unfolded YFP in the bacterial cytoplasm (16). It is known that green fluorescent protein folding in vivo involves chaperones

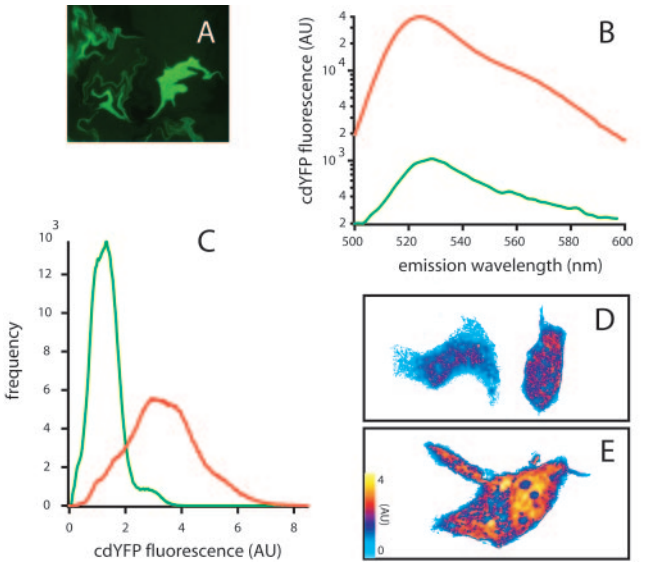

FIG. 3. Characterization of cdYFP folding efficiencies in bacterial and mammalian expression systems. (A) Bacterial folding phenotype, as observed in BL21(DE3) bacterial colonies of retransformed cdYFP mutant cDNA. The marble-like distribution of fluorescent bacteria in the background of bacteria with low or no fluorescence is caused by the induction of the bacterial chaperone program, which is transferred to daughter cells. (B) Cold ethanol shock increases the generation of fluorescence in liquid bacterial cultures by a factor of 40. Red trace, cold ethanol shock; green trace, untreated cells. Excitation was performed at 480 nm, and the emission spectrum for the indicated spectral range is shown. AU, arbitrary units. (C) Distribution of fluorescence expression in CHO cells maintained at 37°C (green trace) or 25°C (red trace). Shown is the cumulative histogram for 10 cells for both traces. The curves were normalized to the sum area of the cells investigated, so that the area under the curve is equal to one. cdYFP fluorescence was normalized so that the maximum emission of cdYFP at 25°C is equal to one. (D) Generation of fluorescent cdYFP by foldase activity in representative cells grown at 37°C. (E) Generation of fluorescent cdYFP emission in a representative cell grown at 25°C. Color coding is shown in the bar; fluorescence emission normalization is equal to that in panel C.

and that green fluorescent protein variants follow different folding trajectories (29). The increased dependence of cdYFP folding on chaperone activity was confirmed by the fact that the fluorescence yield was greatly increased by the induction of chaperones in liquid bacterial cultures after cold ethanol shock (42), which gave rise to an ~40-fold increase in fluorescence yield (Fig. 3B) and the appearance of a clear peak at the YFP chromophoric position (514 nm) in the absorption spectrum of the treated bacteria that was undetectable under noninduction conditions (data not shown).

To allow expression in mammalian cells, cdYFP was subcloned under the control of the cytomegalovirus promoter. Transient expression at 37°C in CHO cells resulted in the homogeneous distribution of low fluorescence intensities in different cells (Fig. 3C, green trace, and Fig. 3D). This finding shows that the overexpression of poorly folded cdYFP by itself is not sufficient to significantly upregulate mammalian chaperone activity. Expression at a low temperature (25°C), in order to relax folding constraints, resulted in a three- to fourfold increase in fluorescence (Fig. 3C, red trace, and Fig. 3E). This finding confirms the impaired folding pathway of cdYFP.

Sequencing analysis of cdYFP selected for our study revealed a glycine-to-serine substitution at amino acid position 32 of YFP. This position is located near the end of the second β strand of the barrel. The 11-β-strand barrel surrounding the central α helix that contains the chromophore represents a difficult folding task. The correct conformation of the second β-strand end and presumably the transition into the third β strand through only a small loop are apparently critical for the correct formation of the entire barrel, which shields the chromophore and provides the proper amino acid side chain context for the chemical formation of the chromophore. Chaperone-mediated folding at this critical initial part of the YFP polypeptide corrects the gross structural defect in the barrel and allows the YFP structure to settle into a form that can accommodate fluorescence. To determine the concentration-independent folding efficiency of cdYFP under various experimental conditions, a concentration reference fluorophore was introduced. In one implementation, an HA epitope was introduced at the cdYFP C terminus to yield HA-cdYFP. The total concentrations of expressed fluorescent cdYFP and nonfluorescent cdYFP can be determined from the fluorescence emission intensity of a Cy5-labeled secondary antibody. This method is used to obtain the distribution and relative concentration of folded cdYFP by image division. In an alternative implementation of the folding sensor, CFP is coexpressed to serve as a reference fluorophore. The advantage over antibody staining is that this assay can be used in living cells, but at the cost of quantification accuracy, as the levels of translated CFP and cdYFP cannot be precisely controlled. We used the quasi-quantitative coexpression method of magnet-assisted transfection and found essentially identical results for the measurements described below, but with higher noise contents and cell-to-cell variations (data not shown). For the antibody reference, the reference is on the same molecule as the folding fluorophore, giving rise to robust and sensitive signals.

To show the sensitivity of the HA-cdYFP folding biosensor to the major mammalian chaperone Hsp70, we compared the folding efficiency of the sensor in wild-type CHO cells with that obtained upon transient coexpression of CFP-Hsp70. In wild-type cells, a single prominent folding peak was observed (Fig. 4A, green trace, and Fig. 4C). Coexpression of Hsp70 in CHO cells resulted in a dramatic increase in the folding ratio (Fig. 4A, red trace, and Fig. 4D), with a skewed distribution to a very high ratio. The use of CFP-Hsp70 allowed us to relate the levels of expression of Hsp70 to the folding efficiency on a cell-by-cell basis. The emission of CFP-Hsp70 can be collected without interference from the higher-wavelength fluorophores used with the foldase sensor (YFP and Cy5) and provides a measurement of the levels of expression of the chaperone. The distributions of folding activity and the levels of expression were plotted against each other to reveal a clearly correlated relationship (Fig. 4B). This experiment demonstrates that the foldase assay reports on the level of Hsp70 chaperone foldase activity in intact cells.

BAG1-mediated folding response. We next proceeded to compare the effects of stable overexpression of BAG1 and its C-terminal deletion mutant, BAGΔC, in CSM14.1 nigral cells (Fig. 5). Wild-type CSM14.1 cells exhibit the same narrow distribution of relatively low cdYFP fluorescence as untreated wild-type CHO cells (Fig. 3C, green trace). The overexpression

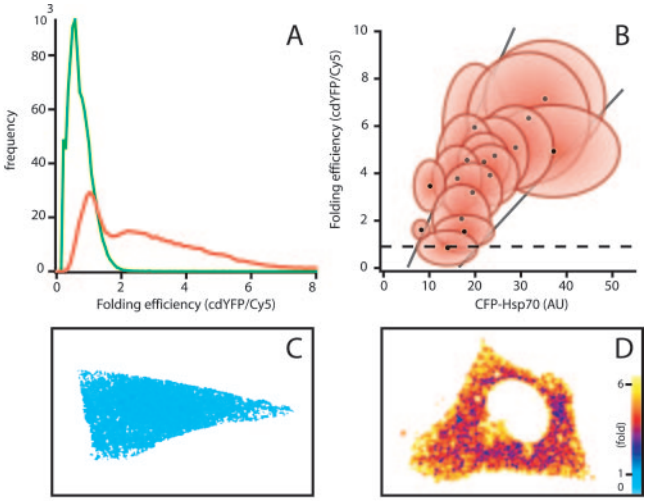

FIG. 4. Dependence of cdYFP folding in mammalian cells on Hsp70. (A) Generation of fluorescent cdYFP in wild-type CHO cells (green trace) and CHO cells transiently expressing Hsp70 (red trace). Shown is the cumulative histogram for 16 cells for both traces. The curves were normalized to the sum area of the cells investigated, so that the area under the curve is equal to one. cdYFP folding efficiency, as expressed by the ratio of cdYFP fluorescence to Cy5-labeled anti-HA antibody immunofluorescence, was normalized to the position of the major folding peak representing partially folded cdYFP in wild-type, untreated cells, as identified by comparison with other experiments. This intermediate can be seen as a separate peak in the red trace and a high-end shoulder in the green trace at a folding efficiency of one. (B) Two-dimensional histogram of the distribution of folding efficiency versus the distribution of CFP-Hsp70 expression, as judged by the fluorescence emission of the conjugated CFP fluorophore, on a cell-by-cell basis for all 16 cells used to construct the red trace in panel A. AU, arbitrary units. (C) cdYFP folding efficiency in a representative wild-type CHO cell. (D) cdYFP folding efficiency in a representative cell expressing Hsp70. Color coding is shown in the bar; folding efficiency normalization is equal to that in panel A.

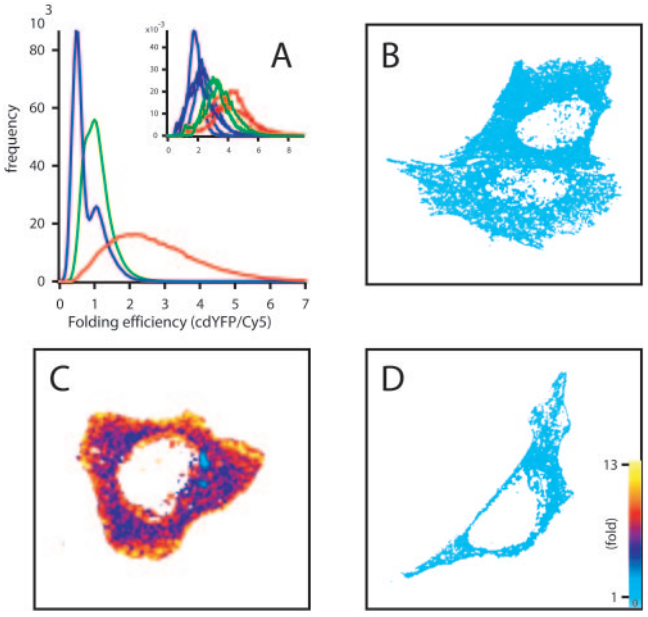

FIG. 5. The cdYFP folding sensor demonstrates the increase in chaperone activity caused by the overexpression of BAG1 in CSM14.1 cells. (A) Generation of fluorescent cdYFP in wild-type CSM14.1 cells (green trace), CSM14.1 cells stably expressing BAG1 (red trace), and CSM14.1 cells stably expressing BAGΔC (blue trace). Shown is the cumulative histogram for 10 cells for all traces. Normalization of folding efficiency and frequency is the same as that in Fig. 4. The inset shows the individual traces for the 10 cells that were used to construct the red trace. These traces were color coded to discriminate cells exhibiting lower folding (blue), intermediate folding (green), and high folding (red) activities in the population of CSM14.1 cells stably expressing BAG1. (B) cdYFP folding efficiency in a representative wild-type CSM14.1 cell. (C) cdYFP folding efficiency in a representative CSM14.1 cell stably expressing BAG1. (D) cdYFP folding efficiency in a representative CSM14.1 cell stably expressing BAGΔC. Color coding is shown in the bar; folding efficiency normalization is equal to that in panel A.

of full-length BAG1 protein dramatically changed this distribution; a new, broad, and high folding efficiency distribution was detected in CSM14.1 cells (Fig. 5A, red trace). The majority of folded cdYFP exhibited an ~2.5-fold increase in fluorescence, but the folding efficiency ranged to as much as a 7-fold increase over that seen in the wild-type situation. The same effect held true for human SHSY-5Y cells stably transfected with BAG1 (Fig. 6, red trace) compared to wild-type SHSY-5Y cells (green trace). This shift was comparable in magnitude to the effect obtained with transient, high-level overexpression of Hsp70, indicating the physiological significance of the regulatory effect of BAG1 on Hsp70. This broad folding efficiency distribution is due to the presence of differently folded intermediates in the analyzed cells. The inset in Fig. 5A shows the presence of discrete distributions among BAG1-overexpressing cells that contain cdYFP, indicative of different equilibria between folding intermediates generated by variations in foldase activities between cells. These consist of species with ~2-fold (Fig. 5A, inset, blue curves), ~3- to 4-fold (green curves), and ~4- to 5-fold (red curves) average increases in folding activities. The BAGΔC mutant, lacking Hsp70 binding capacity, failed to produce this increased folding response in stably expressing CSM14.1 cells (Fig. 5A, blue trace). This result demonstrates the critical importance of the integrity of the BAG binding domain for the chaperone activity of BAG1. In fact, the folding efficiency distribution of the BAGΔC mutant showed a bimodal distribution, with a small peak overlapping the positions of untreated and wild-type cells (green traces in Fig. 3C and 5A) and a new, major peak at a lower folding efficiency (~0.8).

We assign the recurring prominent peak in untreated and native cells to a stable folding intermediate towards properly folded cdYFP (which we normalized to 1). The new low-efficiency peak observed in the BAGΔC mutant, which is also present as a shoulder in the untreated and native folding traces, represents the most poorly folded intermediate that can be assigned in cells. We assign folding ratios of >2 to more fully folded forms. These forms are observed only upon active induction of cellular folding activities, indicating that the endogenous chaperone activity apparently does not suffice to process cdYFP beyond the first partial folding step. The foldase activity needed for further folding obviously exceeds that which is natively present. Upon induction of chaperone activity, both by Hsp70 overexpression or by modulation of endogenous Hsp70 via BAG1 overexpression, the folding pathway apparently diverges to allow for graded "tuning" of folding

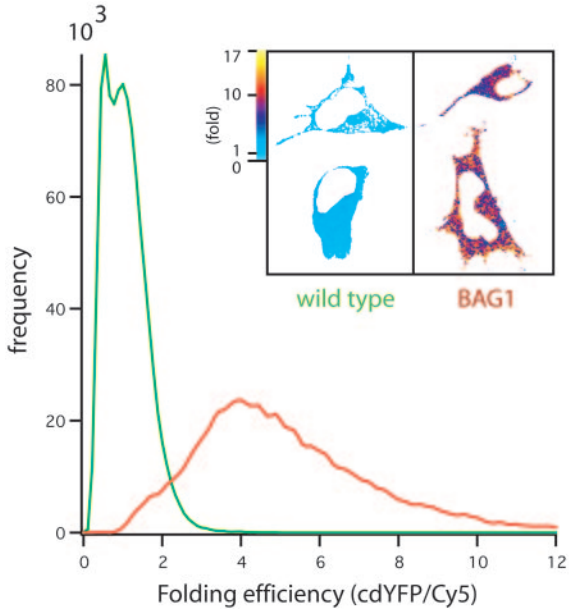

FIG. 6. The cdYFP folding sensor demonstrates the increase in chaperone activity caused by the overexpression of BAG1 in SHSY-5Y cells. The graph shows the generation of fluorescent cdYFP in wild-type SHSY-5Y cells (green trace) and SHSY-5Y cells stably expressing BAG1 (red trace). Shown is the cumulative histogram for 10 cells for all traces. Normalization of folding efficiency and frequency is the same as that in Fig. 4 and 5. The inset shows a representative wild-type cell (left) and a representative transfected cell stably expressing BAG1 (right). Color coding is shown in the bar; folding efficiency normalization is equal to that in the graph.

forms, giving rise to a broad folding efficiency spectrum with various forms possessing low, intermediate, and high folding efficiencies.

Only ~25% of cdYFP is partially folded in BAGΔC-expressing cells, in comparison to >90% for wild-type cells. This finding implies that truncation of the BAG domain generates a strong dominant-negative phenotype with respect to folding, since folding activity is almost completely impaired.

BAGΔC abolishes BAG1-dependent neuroprotection. Having established the BAG1-dependent induction of chaperone activity in rat CSM14.1 and SHSY-5Y cells, we were interested in how the phenotype of these cells is changed when they stably express the deletion mutant BAGΔC, which is no longer capable of inducing this activity (see above). We first examined BAG1 neuroprotectivity. Treatment of CSM14.1 cells with the phospholipid- and calcium-dependent protein kinase inhibitor staurosporine induces mainly apoptotic cell death. At 24 to 48 h, 20 to 40% of wild-type cells survived staurosporine treatment (Fig. 7A). CSM14.1 cells stably overexpressing BAGΔC did not exhibit increased cell survival rates, whereas overexpression of full-length BAG1 significantly protected against staurosporine-induced cell death (Fig. 7B), as shown previously for serum deprivation (19). In a second experimental approach, we applied thapsigargine, a potent IP3-independent intracellular calcium releaser which is known to induce apoptosis. At 48 h, approximately 60% of wild-type cells had undergone apoptosis, which was effectively prevented in cells stably overexpressing BAG1. In contrast, stable expression of BAGΔC did not yield any significant difference in cell survival compared to that seen in wild-type CSM14.1 cells (Fig. 7B). Therefore, BAG1 neuroprotectivity strongly correlates with its ability to induce chaperone activity in intact cells. Because we hypothesized that Hsp70 is a major chaperone mediating BAG1 neuroprotectivity, we examined whether Hsp70 exerts protectivity in our model. To this end, we transiently transfected CSM14.1 cells either with an empty CFP expression vector or with a plasmid containing rat Hsp70 tagged with CFP at the N terminus. As illustrated in Fig. 7, Hsp70 substantially inhibited staurosporine toxicity.

Since it is still a matter of debate and controversy whether BAG1 neuroprotectivity is dependent on the inhibition of caspase activation, we finally wanted to know whether BAG1 overexpression—being highly protective in our model—is accompanied by decreased levels of activity of caspase 3, one of the main effectors of apoptosis in neurons. Surprisingly, we found no difference in caspase 3 activation 12 h after staurosporine treatment in BAG1-overexpressing cells compared to their wild-type counterparts (Fig. 7D).

BAGΔC still accelerates the differentiation of CSM14.1 cells. As described previously for cells overexpressing full-length BAG1, we observed morphological changes in BAGΔC-overexpressing cells already at the permissive temperature of 32°C. In contrast to the small and round shape of wild-type cells, BAGΔC-overexpressing cells are larger and display a more polarized shape, suggesting an increased cytosol/nucleus ratio. To induce differentiation in our stable cell lines, we switched the culture temperature from 32 to 39°C (19, 51).

To further explore the effects of BAGΔC on neuronal differentiation, we first measured the length of axon-like processes. After 8 days of culturing at the nonpermissive temperature, only a few wild-type cells had grown processes. BAG1- and BAGΔC-overexpressing cells had consistently grown long processes and formed nests with axon-like networks. Measurement of the lengths of these processes revealed a highly significant increase in these cells compared to wild-type cells ($P < 0.001$) (Fig. 8A).

Second, we evaluated the doubling times of CSM14.1 cell transfectants expressing BAG1 or BAGΔC. As in BAG1-overexpressing cells (19), there was a highly significant difference in the generation times of BAGΔC-expressing cells and wild-type cells at 32°C ($P < 0.001$). BAGΔC-transfected cells were less proliferative, with an average generation time of 41 h, similar to BAG1-overexpressing cells. In contrast, wild-type CSM14.1 cells doubled, on average, every 25 h (Fig. 8B).

Third, to correlate these changes in axon length and proliferation with neuronal differentiation, we also investigated the expression of the NeuN neuronal differentiation marker in these cells. Again, in agreement with findings for cells expressing full-length BAG1, we detected positive NeuN staining after 22 days of culturing at the nonpermissive temperature in most cells overexpressing BAGΔC, while NeuN staining remained absent in CSM 14.1 control cells (Fig. 8C). We conclude therefore that BAGΔC retains its ability to promote neuronal differentiation, despite lacking cochaperone activity.

One may speculate that these observations are a consequence of the interaction of BAG1 with Raf-1 kinase. Thus, we finally checked whether BAGΔC, like BAG1 (18), still induces Raf-1-dependent Erk phorphorylation. As shown in

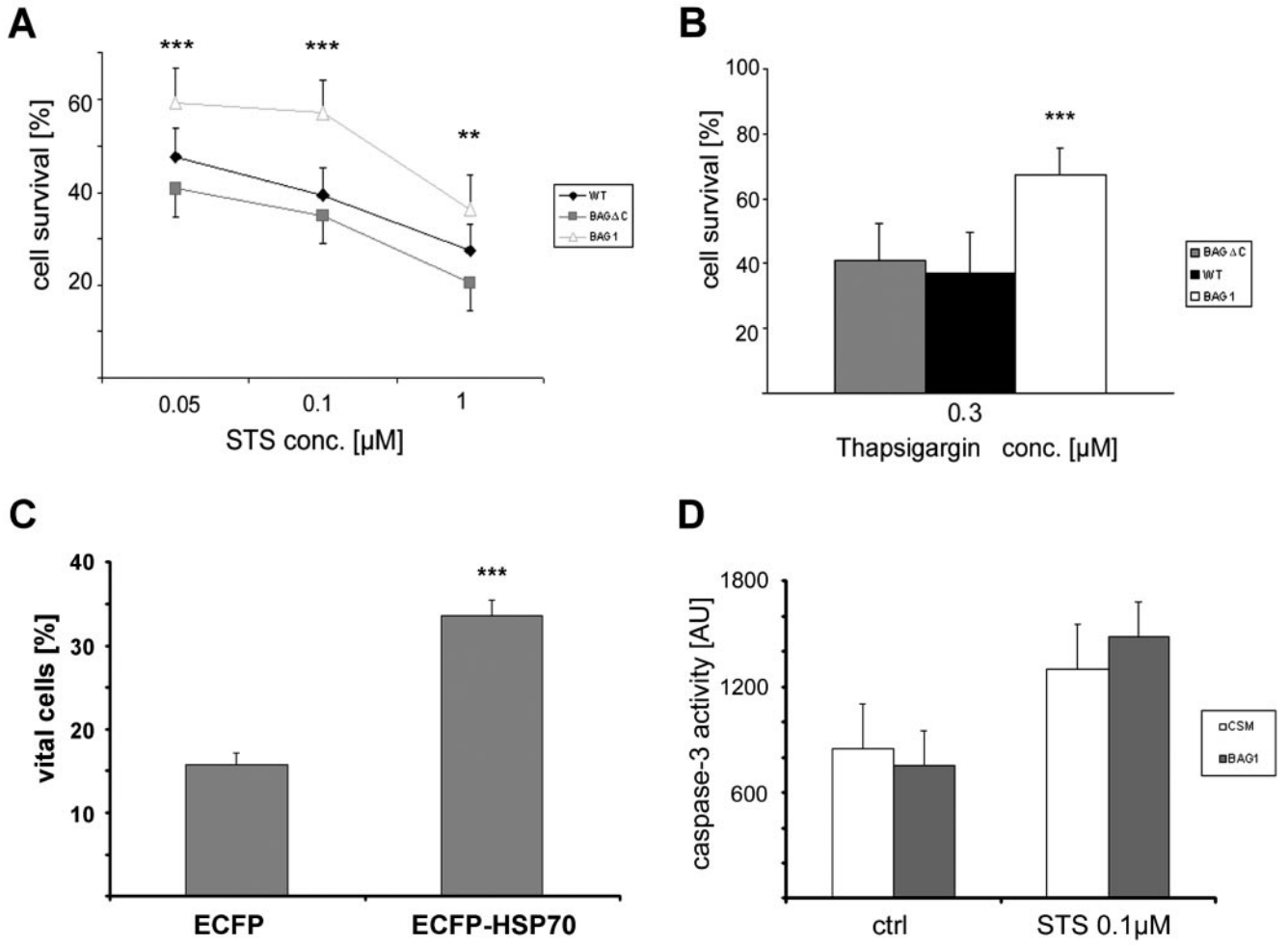

FIG. 7. BAGΔC does not protect against staurosporine (STS)- or thapsigargine-induced cell death, while Hsp70 is highly neuroprotective. (A) CSM14.1 cells were treated with increasing concentrations of staurosporine for 48 h ($n = 6$; mean ± standard error of the mean [SEM]; double and triple asterisks indicate P values of <0.01 and <0.001, respectively). Overexpression of full-length BAG1 resulted in highly significant protection against staurosporine-induced toxicity, while cells overexpressing BAGΔC were not protected but showed a trend toward even higher susceptibility to staurosporine toxicity than wild-type (WT) cells. (B) CSM14.1 cells were treated with 0.3 μM thapsigargine for 48 h ($n = 6$; mean ± standard deviation [SD]; triple asterisks indicate a P value of <0.001). While BAG1-overexpressing cells exhibited strong resistance against ER stress, cells overexpressing BAGΔC and wild-type cells did not. (C) CSM14.1 cells were transiently transfected with ECFP-Hsp70, and cell survival was assessed after treatment with staurosporine as described for panel A. A total of 1,000 green cells from three independent experiments were evaluated by two investigators as vital or dead (mean ± SEM; triple asterisks indicate a P value of <0.001). Hsp70 overexpression proved to be highly protective. (D) Caspase 3 activity was measured in a fluorogenic assay for CSM14.1 (CSM) wild-type and BAG1-expressing cells with or without 0.1 μM staurosporine challenge for 12 h ($n = 4$; mean ± SD). While staurosporine treatment induced marked caspase 3 activity, no significant difference between wild-type and BAG1-expressing cells could be documented. AU, arbitrary units; ctrl, control.

Fig. 8D, phosphorylated Erk1/2 levels were similarly increased in cells overexpressing BAG1 and BAGΔC compared to wild-type cells.

DISCUSSION

BAG1 has been characterized as a regulator and marker of neuronal differentiation exhibiting neuroprotective properties in vitro as well as in a transgenic mouse model in vivo (18, 19). This multifunctionality has been suggested to be dependent on the binding partners interacting with BAG1 (37). To explore the influence of the known binding partner Hsp70 on the above-mentioned features of BAG1, in the present study we stably overexpressed BAGΔC, which was previously reported to lack Hsp70 binding capacity (34). We used CSM14.1 cells, which originate from rat nigrostriatal neurons immortalized by expression of the temperature-sensitive simian virus 40 large T antigen. These cells show a high proliferation rate at a permissive temperature, while the inactivation of large T antigen at a nonpermissive temperature induces neuronal differentiation (51).

BAG1 but not BAGΔC increases chaperone activity in living cells. It is known that chaperones interact with misfolded or partially folded polypeptides in order to prevent interactions that would result in aggregation. Chaperones belonging to the Hsp70 family process the majority of substrates within the eukaryotic cytosol. The main function of these chaperones is to fold newly synthesized proteins or to refold proteins after

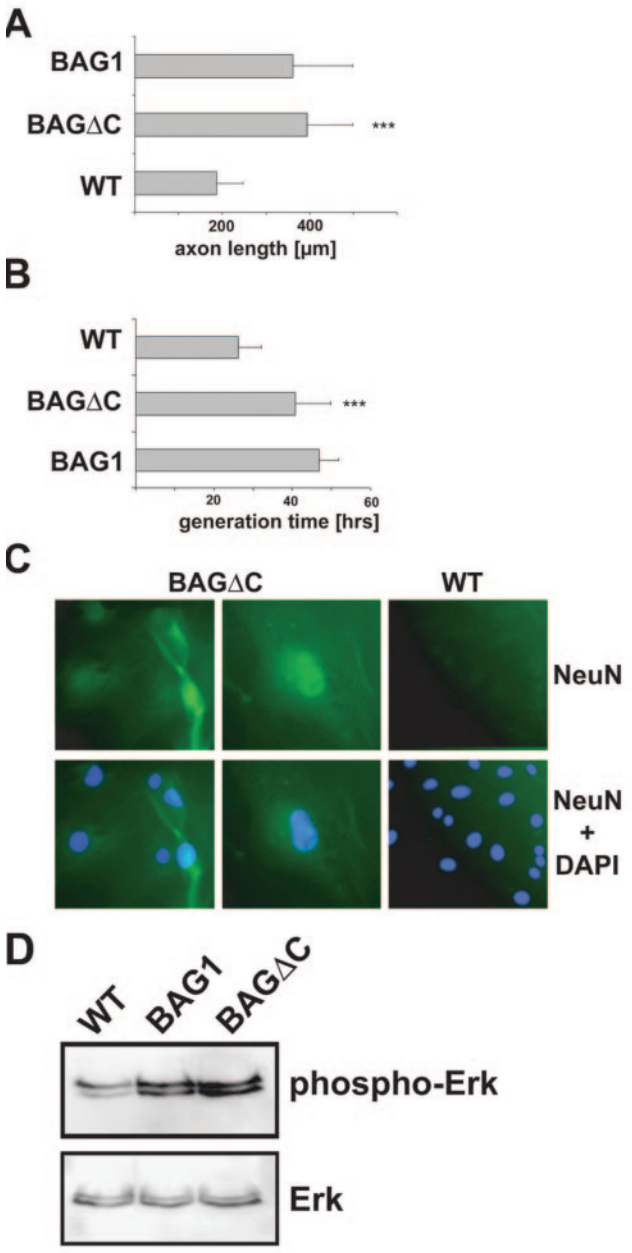

FIG. 8. BAGΔC still induces neuronal differentiation in vitro. (A) Measurement of neurite extension in BAGΔC-overexpressing versus BAG1-overexpressing and wild-type (WT) cells (70 cells measured in three independent experiments; mean ± standard deviation [SD]). Note that neurites in BAGΔC- and full-length BAG1-overexpressing cells were significantly longer than those in wild-type cells (triple asterisks indicate a P value of <0.001). (B) Generation time assessed by counting cell numbers during logarithmic growth at a permissive temperature (32°C) over 1 week ($n = 6$). Average generation time (mean ± SD) was significantly longer in BAGΔC- and full-length BAG1-overexpressing cells than in wild-type cells (triple asterisks indicate a P value of <0.001). (C) BAGΔC-overexpressing cells (left and middle panels; magnifications, ×200 and ×400, respectively) and wild-type cells (right panels; magnification, ×200) after 22 days at a nonpermissive temperature were stained with fluorescein isothiocyanate-labeled NeuN and counterstained with DAPI. BAGΔC-overexpressing cells displayed nuclear expression of the differentiation marker NeuN, which was absent in wild-type cells. (D) Cells overexpressing BAG1 or BAGΔC showed similarly elevated levels of phosphorylated Erk1/2 expression compared to wild-type cells.

stress denaturation through ATP binding and hydrolysis (6, 12, 48). The subcellular localization and the substrates of such chaperones are predominantly determined by a number of regulatory or accessory cochaperones. In general, such cochaperones consist of a chaperone binding domain and other domains involving different activities or localizations within cells. BAG1 is one of those known cochaperones. It has a C-terminal BAG domain which binds mainly by electrostatic interactions to Hsp70 (33). BAG1 binds to the ATPase domain of Hsp70, resulting in a potent acceleration of ATPase activity (13). Further investigations revealed that this acceleration is due to the stimulation of ADP release via opening of the nucleotide binding cleft of the Hsp70 ATPase domain (10, 13, 33). BAG1 thereby acts as a nucleotide exchange factor for Hsp70, triggering substrate unloading from the chaperone. Although the mechanism of the BAG1-Hsp70 interaction has been studied extensively, the influence of BAG1 on chaperone foldase activity is still a subject of controversy and debate. While some studies suggested BAG1 to be an inhibitor of ATP-dependent Hsp70 activity (11, 36, 49), others presented strong opposing evidence for BAG1 as a stimulatory cochaperone (10, 41). These opposing findings were attributed to differences in cofactor expression but also to the expression of various BAG1 isoforms, with the short forms of BAG1 acting as positive regulators and the longer forms acting as negative regulators of chaperone foldase activity (22).

In this study, we demonstrated that the short isoform of mouse BAG1 dramatically increases chaperone foldase activity in neurons. This effect is species independent, since we observed it in rodent and human neuronal cells. To our knowledge, we are the first to demonstrate and quantify BAG1-dependent chaperone activity directly inside single cells in situ. These results were achieved by the generation of a novel folding-impaired YFP mutant whose folding dependence on chaperones is tuned such that it can be used as an effective sensor for cellular foldase activity. This cdYFP indicator protein can leave its intrinsically misfolded, nonfluorescent state upon correct refolding by cellular chaperones, thereby regaining detectable fluorescence. As an example, we showed the responsiveness of the cdYFP folding reaction to the major chaperone Hsp70. Other chaperones, such as Hsc70, which has also been implicated as a regulatory target for BAG1, are likely to contribute to correct cdYFP folding in case they are upregulated by BAG1 overexpression. By use of a spectrally different fluorescent concentration reference, a sensitive and reproducible sensor for cellular chaperone activity was achieved. This sensor allowed departure from conventional "artificial" extracellular activity assays, with all their procedural pitfalls, to observe chaperone activity through the microscope in intact cells in situ. The applicability of this novel sensor is underscored by our observation of discrete equilibria of the process of refolding of a misfolded protein in single cells. We therefore believe that the cdYFP sensor can be generally used for protein folding and refolding analyses beyond the scope of the present study.

In our experimental paradigm, wild-type rat CSM14.1 and human SHSY-5Y cells, as well as CHO cells, show a single prominent peak of folding activity. By comparison of the dif-

ferent treatments, this peak could be assigned to a stable folding intermediate. Experiments with BAGΔC-expressing cells showed the presence of a further folding intermediate with a lower efficiency. In retrospect, the lower-efficiency shoulders of the folding efficiency distributions of wild-type and untreated cells could be seen to contain a fraction of this poorly folded "base" condition of the sensor (Fig. 4A, green trace versus red trace, and Fig. 5A). Wild-type cells are not able to overcome the "second" step in protein refolding. In contrast, cells stably overexpressing BAG1 or Hsp70 directly show a prominent high-efficiency distribution indicating further advanced protein refolding. This distribution is broader and less symmetrical than the poorly and initially folded distribution. These high-folding activity distributions, when compared on a cell-by-cell basis, demonstrate the progressive dependence on the folding threshold on Hsp70 expression levels (Fig. 4B) and on discrete fine-tuning steps at more advanced refolding activities, e.g., upon BAG1 overexpression (Fig. 5A, inset). Surprisingly, BAGΔC, which lacks the Hsp70 binding C terminus, does not yield results similiar to those seen in wild-type CSM14.1 cells but seems to impair protein refolding even further. This observation is in line with results obtained by Gassler et al. (10), who measured the influence of BAG1 and a C-terminal deletion mutant of BAG1 on Hsp70 ADP turnover. They found an ~900-fold increase in ADP turnover in cells transfected with BAG1, whereas cells transfected with the deletion mutant displayed a 4-fold decrease (10). This effect was explained by the presence of an additional domain which is situated in an N-terminal location relative to the BAG domain, which is apparently important for the binding and activation of chaperones, and which acts in a dominant-negative manner on chaperone foldase activity.

An interaction between Hsp70 and BAG1 is necessary for the neuroprotective effect but not for neuronal differentiation. The results discussed above posed the question of how BAG1 exerts its antiapoptotic activity and which protein interactions are necessary. It has been suggested that the linkage of BAG1 to the proteasome and its interaction with Hsp70 are important for cell survival in breast cancer cells and cardiomyocytes (43, 44).

In our study, CSM14.1 cells overexpressing BAGΔC, like wild-type cells but unlike BAG1-overexpressing cells, remained sensitive to apoptotic stimuli induced by staurosporine and thapsigargine. Since BAGΔC cannot bind to Hsp70 and lacks chaperone activity, it is likely that the neuroprotective effect of full-length BAG1 in neurons is the result of the modulation of Hsp70 chaperone activity. Obviously, we cannot rule out the possibility that chaperones other than Hsp70 are bound and activated through the BAG domain of BAG1 and contribute to BAG1 neuroprotectivity. However, if the cytoprotective effect of BAG1 depends on Hsp70 activation, then Hsp70 by itself should exert neuroprotectivity in our experimental paradigm. In accordance with this notion, we show here that Hsp70 substantially blocks staurosporine toxicity. A proposed mechanism for the antiapoptotic effect of BAG1 via Hsp70 is suggested by other experiments, where it was found that the interaction of Hsp70 with Apaf-1 prevents the formation of the apoptosome, thereby averting the enforcement of the intrinsic apoptosis pathway (3, 30). However, the precise mechanism by which apoptosis is abolished still remains to be elucidated, and it may not be assigned to the action of a single protein, such as Apaf-1. For example, Hsp70 has also been shown to protect cells from enforced caspase 3 expression. This finding indicates that Hsp70 is also able to block apoptosis downstream of apoptosome-dependent caspase activation (14). In line with the latter results, we did not observe significant differences in caspase 3 activation 12 h following staurosporine treatment in wild-type and BAG1-overexpressing cells.

Since we demonstrated a highly significant upregulation of chaperone foldase activity in this study, we suggest that the interaction of BAG1 and Hsp70 is the key mechanism for delivering the neuroprotective effect of BAG1 by serving as a positive regulator of Hsp70 foldase activity in neurons. In this regard, not only is Hsp70 known to be a neuroprotectant in the context of ischemic neuronal death (8, 17, 21, 26, 27, 40), but also it is known to suppress neuropathology in mouse models of polyglutamine repeat diseases, including spinocerebellar ataxia (7) and Huntington's disease (15), as well as in amyotrophic lateral sclerosis (5, 46). Since the three-dimensional structure of the BAG1-Hsp70-ATPase domain complex has been solved (33) and critical contact sites have been mapped for BAG1 binding and cochaperone activities (4), it is conceivable that small-molecule drugs that would have neuroprotective properties and that would occupy the BAG1 binding site on the ATPase domain of Hsp70 could be identified. These drugs would act as BAG1 mimics, thereby enhancing Hsp70 function. Additionally, BAG1 cDNAs might be considered for use in gene therapy applications for neurological diseases where cell loss represents the underlying pathological event.

Apart from the interaction of BAG1 with Hsp70, multiple BAG1 functions and interaction partners have been ascertained; these include the binding and activation of Raf-1 kinase, the regulation of proteasomal degradation, and differentiation-accelerating effects (1, 9, 19, 34, 38, 45). It appears that an additional feature of the BAG1 protein is regulation of the cell cycle and proliferation. BAG1-overexpressing neurons, as well as human breast cancer cells, show signs of a prolonged cell cycle, with reduced proliferation but increased differentiation (19, 20, 23, 28, 34). Moreover, it has been suggested that BAG1 is of importance for the developing nervous system. The p29 BAG1 isoform used in this study has been reported to localize mostly to the nucleus (19, 24). However, there is a characteristic shift from mainly nuclear expression in proliferating neurons to mostly cytosolic expression in differentiating neurons in the mouse brain and in cell cultures (18), with BAGΔC being exclusively found in the cytosol (this study). Furthermore, $BAG1^{-/-}$ mice died by embryonic day 13 and showed marked disturbances of cortical layering (47).

Thus, in the present study, we were also interested in the influence of the Hsp70-BAG1 interaction on cellular differentiation. We assessed neuronal differentiation in CSM14.1 cells expressing BAGΔC, wild-type cells, and cells overexpressing full-length BAG1. Interestingly, the accelerating effect of BAG1 on neuronal differentiation was independent of its binding to Hsp70. These cells displayed identical features of neuronal differentiation. One may speculate that these observations are a consequence of the interaction of BAG1 with Raf-1 kinase. Raf-1 kinase is crucially involved in cellular proliferation and differentiation (25) and has been shown to slow pro-

liferation and increase differentiation in certain cell lineages, particulary neuronal progenitors and tumor-derived cells (32). BAG1 binds to Raf-1 kinase and increases its activity (34, 45). In this study, we showed that the levels of Raf-1-mediated Erk phosphorylation were similarly elevated in cells overexpressing full-length BAG1 or BAGΔC. Thus, Raf-1 kinase appears to be a promising focus for future experimental efforts to further dissect the cellular pathways modulated by BAG1.

ACKNOWLEDGMENTS

This investigation was supported by a starter grant from the University of Goettingen (to P.K.), the graduate college GRK 723 Spatio-Temporal Signal Processes in Neurons and Cellular Biophysics (to S.G.), the DFG Research Center Molecular Physiology of the Brain (to P.K. and F.S.W.), and CA67329 (to J.C.R.).

REFERENCES

1. **Alberti, S., J. Demand, C. Esser, N. Emmerich, H. Schild, and J. Hohfeld.** 2002. Ubiquitylation of BAG-1 suggests a novel regulatory mechanism during the sorting of chaperone substrates to the proteasome. J. Biol. Chem. **277:**45920–45927.
2. **Bardelli, A., P. Longati, D. Albero, S. Goruppi, C. Schneider, C. Ponzetto, and P. M. Comoglio.** 1996. HGF receptor associates with the anti-apoptotic protein BAG-1 and prevents cell death. EMBO J. **15:**6205–6212.
3. **Beere, H. M., B. B. Wolf, K. Cain, D. D. Mosser, A. Mahboubi, T. Kuwana, P. Tailor, R. I. Morimoto, G. M. Cohen, and D. R. Green.** 2000. Heat-shock protein 70 inhibits apoptosis by preventing recruitment of procaspase-9 to the Apaf-1 apoptosome. Nat. Cell Biol. **2:**469–475.
4. **Briknarova, K., S. Takayama, L. Brive, M. L. Havert, D. A. Knee, J. Velasco, S. Homma, E. Cabezas, J. Stuart, D. W. Hoyt, A. C. Satterthwait, M. Llinas, J. C. Reed, and K. R. Ely.** 2001. Structural analysis of BAG1 cochaperone and its interactions with Hsc70 heat shock protein. Nat. Struct. Biol. **8:**349–352.
5. **Bruening, W., J. Roy, B. Giasson, D. A. Figlewicz, W. E. Mushynski, and H. D. Durham.** 1999. Up-regulation of protein chaperones preserves viability of cells expressing toxic Cu/Zn-superoxide dismutase mutants associated with amyotrophic lateral sclerosis. J. Neurochem. **72:**693–699.
6. **Bukau, B., and A. L. Horwich.** 1998. The Hsp70 and Hsp60 chaperone machines. Cell **92:**351–366.
7. **Cummings, C. J., Y. Sun, P. Opal, B. Antalffy, R. Mestril, H. T. Orr, W. H. Dillmann, and H. Y. Zoghbi.** 2001. Over-expression of inducible HSP70 chaperone suppresses neuropathology and improves motor function in SCA1 mice. Hum. Mol. Genet. **10:**1511–1518.
8. **Currie, R. W., J. A. Ellison, R. F. White, G. Z. Feuerstein, X. Wang, and F. C. Barone.** 2000. Benign focal ischemic preconditioning induces neuronal Hsp70 and prolonged astrogliosis with expression of Hsp27. Brain Res. **863:**169–181.
9. **Demand, J., S. Alberti, C. Patterson, and J. Hohfeld.** 2001. Cooperation of a ubiquitin domain protein and an E3 ubiquitin ligase during chaperone/proteasome coupling. Curr. Biol. **11:**1569–1577.
10. **Gassler, C. S., T. Wiederkehr, D. Brehmer, B. Bukau, and M. P. Mayer.** 2001. Bag-1M accelerates nucleotide release for human Hsc70 and Hsp70 and can act concentration-dependent as positive and negative cofactor. J. Biol. Chem. **276:**32538–32544.
11. **Gebauer, M., M. Zeiner, and U. Gehring.** 1997. Proteins interacting with the molecular chaperone hsp70/hsc70: physical associations and effects on refolding activity. FEBS Lett. **417:**109–113.
12. **Hartl, F. U., and M. Hayer-Hartl.** 2002. Molecular chaperones in the cytosol: from nascent chain to folded protein. Science **295:**1852–1858.
13. **Hohfeld, J., and S. Jentsch.** 1997. GrpE-like regulation of the hsc70 chaperone by the anti-apoptotic protein BAG-1. EMBO J. **16:**6209–6216.
14. **Jaattela, M., D. Wissing, K. Kokholm, T. Kallunki, and M. Egeblad.** 1998. Hsp70 exerts its anti-apoptotic function downstream of caspase-3-like proteases. EMBO J. **17:**6124–6134.
15. **Jana, N. R., M. Tanaka, G. Wang, and N. Nukina.** 2000. Polyglutamine length-dependent interaction of Hsp40 and Hsp70 family chaperones with truncated N-terminal huntingtin: their role in suppression of aggregation and cellular toxicity. Hum. Mol. Genet. **9:**2009–2018.
16. **Jurgen, B., H. Y. Lin, S. Riemschneider, C. Scharf, P. Neubauer, R. Schmid, M. Hecker, and T. Schweder.** 2000. Monitoring of genes that respond to overproduction of an insoluble recombinant protein in Escherichia coli glucose-limited fed-batch fermentations. Biotechnol. Bioeng. **70:**217–224.
17. **Kelly, S., A. Bieneman, K. Horsburgh, D. Hughes, M. V. Sofroniew, J. McCulloch, and J. B. Uney.** 2001. Targeting expression of hsp70i to discrete neuronal populations using the Lmo-1 promoter: assessment of the neuroprotective effects of hsp70i in vivo and in vitro. J. Cereb. Blood Flow Metab. **21:**972–981.
18. **Kermer, P., M. H. Digicaylioglu, M. Kaul, J. M. Zapata, M. Krajewska, F. Stenner-Liewen, S. Takayama, S. Krajewski, S. A. Lipton, and J. C. Reed.** 2003. BAG1 over-expression in brain protects against stroke. Brain Pathol. **13:**495–506.
19. **Kermer, P., M. Krajewska, J. M. Zapata, S. Takayama, J. Mai, S. Krajewski, and J. C. Reed.** 2002. Bag1 is a regulator and marker of neuronal differentiation. Cell Death Differ. **9:**405–413.
20. **Kudoh, M., D. A. Knee, S. Takayama, and J. C. Reed.** 2002. Bag1 proteins regulate growth and survival of ZR-75-1 human breast cancer cells. Cancer Res. **62:**1904–1909.
21. **Lee, S. H., M. Kim, B. W. Yoon, Y. J. Kim, S. J. Ma, J. K. Roh, J. S. Lee, and J. S. Seo.** 2001. Targeted hsp70.1 disruption increases infarction volume after focal cerebral ischemia in mice. Stroke **32:**2905–2912.
22. **Luders, J., J. Demand, O. Papp, and J. Hohfeld.** 2000. Distinct isoforms of the cofactor BAG-1 differentially affect Hsc70 chaperone function. J. Biol. Chem. **275:**14817–14823.
23. **Matsuzawa, S., S. Takayama, B. A. Froesch, J. M. Zapata, and J. C. Reed.** 1998. p53-inducible human homologue of Drosophila seven in absentia (Siah) inhibits cell growth: suppression by BAG-1. EMBO J. **17:**2736–2747.
24. **Nollen, E. A., J. F. Brunsting, J. Song, H. H. Kampinga, and R. I. Morimoto.** 2000. Bag1 functions in vivo as a negative regulator of Hsp70 chaperone activity. Mol. Cell. Biol. **20:**1083–1088.
25. **O'Neill, E., and W. Kolch.** 2004. Conferring specificity on the ubiquitous Raf/MEK signalling pathway. Br. J. Cancer **90:**283–288.
26. **Rajdev, S., K. Hara, Y. Kokubo, R. Mestril, W. Dillmann, P. R. Weinstein, and F. R. Sharp.** 2000. Mice overexpressing rat heat shock protein 70 are protected against cerebral infarction. Ann. Neurol. **47:**782–791.
27. **Rokutan, K., T. Hirakawa, S. Teshima, Y. Nakano, M. Miyoshi, T. Kawai, E. Konda, H. Morinaga, T. Nikawa, and K. Kishi.** 1998. Implications of heat shock/stress proteins for medicine and disease. J. Med. Investig. **44:**137–147.
28. **Roth, W., C. Grimmel, L. Rieger, H. Strik, S. Takayama, S. Krajewski, R. Meyermann, J. Dichgans, J. C. Reed, and M. Weller.** 2000. Bag-1 and Bcl-2 gene transfer in malignant glioma: modulation of cell cycle regulation and apoptosis. Brain Pathol. **10:**223–234.
29. **Sacchetti, A., V. Cappetti, P. Marra, R. Dell'Arciprete, T. El Sewedy, C. Crescenzi, and S. Alberti.** 2001. Green fluorescent protein variants fold differentially in prokaryotic and eukaryotic cells. J. Cell. Biochem. **81:**117–128.
30. **Saleh, A., S. M. Srinivasula, L. Balkir, P. D. Robbins, and E. S. Alnemri.** 2000. Negative regulation of the Apaf-1 apoptosome by Hsp70. Nat. Cell Biol. **2:**476–483.
31. **Schulz, J. B., D. Bremen, J. C. Reed, J. Lommatzsch, S. Takayama, U. Wullner, P. A. Loschmann, T. Klockgether, and M. Weller.** 1997. Cooperative interception of neuronal apoptosis by BCL-2 and BAG-1 expression: prevention of caspase activation and reduced production of reactive oxygen species. J. Neurochem. **69:**2075–2086.
32. **Sippel, R. S., and H. Chen.** 2002. Activation of the ras/raf-1 signal transduction pathway in carcinoid tumor cells results in morphologic transdifferentiation. Surgery **132:**1035–1039.
33. **Sondermann, H., C. Scheufler, C. Schneider, J. Hohfeld, F. U. Hartl, and I. Moarefi.** 2001. Structure of a Bag/Hsc70 complex: convergent functional evolution of Hsp70 nucleotide exchange factors. Science **291:**1553–1557.
34. **Song, J., M. Takeda, and R. I. Morimoto.** 2001. Bag1-Hsp70 mediates a physiological stress signalling pathway that regulates Raf-1/ERK and cell growth. Nat. Cell Biol. **3:**276–282.
35. **Takaoka, A., M. Adachi, H. Okuda, S. Sato, A. Yawata, Y. Hinoda, S. Takayama, J. C. Reed, and K. Imai.** 1997. Anti-cell death activity promotes pulmonary metastasis of melanoma cells. Oncogene **14:**2971–2977.
36. **Takayama, S., D. N. Bimston, S. Matsuzawa, B. C. Freeman, C. Aime-Sempe, Z. Xie, R. I. Morimoto, and J. C. Reed.** 1997. BAG-1 modulates the chaperone activity of Hsp70/Hsc70. EMBO J. **16:**4887–4896.
37. **Takayama, S., and J. C. Reed.** 2001. Molecular chaperone targeting and regulation by BAG family proteins. Nat. Cell Biol. **3:**E237–E241.
38. **Takayama, S., T. Sato, S. Krajewski, K. Kochel, S. Irie, J. A. Millan, and J. C. Reed.** 1995. Cloning and functional analysis of BAG-1: a novel Bcl-2-binding protein with anti-cell death activity. Cell **80:**279–284.
39. **Takayama, S., Z. Xie, and J. C. Reed.** 1999. An evolutionarily conserved family of Hsp70/Hsc70 molecular chaperone regulators. J. Biol. Chem. **274:**781–786.
40. **Tanaka, S., K. Kitagawa, T. Ohtsuki, Y. Yagita, K. Takasawa, M. Hori, and M. Matsumoto.** 2002. Synergistic induction of HSP40 and HSC70 in the mouse hippocampal neurons after cerebral ischemia and ischemic tolerance in gerbil hippocampus. J. Neurosci. Res. **67:**37–47.
41. **Terada, K., and M. Mori.** 2000. Human DnaJ homologs dj2 and dj3, and bag-1 are positive cochaperones of hsc70. J. Biol. Chem. **275:**24728–24734.
42. **Thomas, J. G., and F. Baneyx.** 1996. Protein misfolding and inclusion body formation in recombinant Escherichia coli cells overexpressing Heat-shock proteins. J. Biol. Chem. **271:**11141–11147.
43. **Townsend, P. A., R. I. Cutress, C. J. Carroll, K. M. Lawrence, T. M. Scarabelli, G. Packham, A. Stephanou, and D. S. Latchman.** 2004. BAG-1 proteins protect cardiac myocytes from simulated ischemia/reperfusion-induced ap-

optosis via an alternate mechanism of cell survival independent of the proteasome. J. Biol. Chem. **279:**20723–20728.
44. **Townsend, P. A., R. I. Cutress, A. Sharp, M. Brimmell, and G. Packham.** 2003. BAG-1 prevents stress-induced long-term growth inhibition in breast cancer cells via a chaperone-dependent pathway. Cancer Res. **63:**4150–4157.
45. **Wang, H. G., S. Takayama, U. R. Rapp, and J. C. Reed.** 1996. Bcl-2 interacting protein, BAG-1, binds to and activates the kinase Raf-1. Proc. Natl. Acad. Sci. USA **93:**7063–7068.
46. **Watanabe, M., M. Dykes-Hoberg, V. C. Culotta, D. L. Price, P. C. Wong, and J. D. Rothstein.** 2001. Histological evidence of protein aggregation in mutant SOD1 transgenic mice and in amyotrophic lateral sclerosis neural tissues. Neurobiol. Dis. **8:**933–941.
47. **Wiese, S., R. Gotz, W. Rossoll, U. Schweizer, S.Takajama, M. Berzaghi, S. Jablonka, B. Holtmann, J. C. Reed, U. R. Rapp, and M. Sendtner.** 2002. Essential role for BAG-1 in differentiation and survival of neurons, CD-ROM program no. 618.4. Abstract Viewer/Itinerary Planner. Society for Neuroscience, Washington, D.C.
48. **Young, J. C., I. Moarefi, and F. U. Hartl.** 2001. Hsp90: a specialized but essential protein-folding tool. J. Cell Biol. **154:**267–273.
49. **Zeiner, M., M. Gebauer, and U. Gehring.** 1997. Mammalian protein RAP46: an interaction partner and modulator of 70 kDa heat shock proteins. EMBO J. **16:**5483–5490.
50. **Zeiner, M., and U. Gehring.** 1995. A protein that interacts with members of the nuclear hormone receptor family: identification and cDNA cloning. Proc. Natl. Acad. Sci. USA **92:**11465–11469.
51. **Zhong, L. T., T. Sarafian, D. J. Kane, A. C. Charles, S. P. Mah, R. H. Edwards, and D. E. Bredesen.** 1993. bcl-2 inhibits death of central neural cells induced by multiple agents. Proc. Natl. Acad. Sci. USA **90:**4533–4537.